ACADEMIC PRESS

Available online at www.sciencedirect.com
SCIENCE DIRECT®

NeuroImage

NeuroImage 20 (2003) 2100–2118

www.elsevier.com/locate/ynimg

# Development and evaluation of an automated atlas-based image analysis method for microPET studies of the rat brain

Daniel J. Rubins,[a] William P. Melega,[a,*] Goran Lacan,[a] Baldwin Way,[a] Alain Plenevaux,[b] Andre Luxen,[b] and Simon R. Cherry[c]

[a] *Department of Molecular and Medical Pharmacology, David Geffen School of Medicine, University of California, Los Angeles, CA, USA*
[b] *Cyclotron Research Center, Liege University, Liege, Belgium*
[c] *Department of Biomedical Engineering, University of California, Davis, CA, USA*

Received 29 April 2003; revised 18 July 2003; accepted 22 July 2003

**Abstract**

An automated method for placement of 3D rat brain atlas-derived volumes of interest (VOIs) onto PET studies has been designed and evaluated. VOIs representing major structures of the rat brain were defined on a set of digitized cryosectioned images of the rat brain. For VOI placement, each PET study was registered with a synthetic PET target constructed from the VOI template. Registration was accomplished with an automated algorithm that maximized the mutual information content of the image volumes. The accuracy and precision of this method for VOI placement was determined using datasets from PET studies of the striatal dopamine and hippocampal serotonin systems. Each evaluated PET study could be registered to at least one synthetic PET target without obvious failure. Registration was critically dependent upon the initial position of the PET study relative to the synthetic PET target, but not dependent on the amount of synthetic PET target smoothing. An evaluation algorithm showed that resultant radioactivity concentration measurements of selected brain structures had errors = 2% due to misalignment with the corresponding VOI. Further, radioligand binding values calculated from these measurements were found to be more precise than those calculated from measurements obtained with manually drawn regions of interest (ROIs). Overall, evaluation results demonstrated that this atlas-derived VOI method can be used to obtain unbiased measurements of radioactivity concentration from PET studies. Its automated features, and applicability to different radioligands and brain regions, will facilitate quantitative rat brain PET assessment procedures.


## 1. Introduction

Small laboratory animals, primarily the rat and mouse, are commonly used in brain research. A wide range of measurements can be obtained in these animals by terminal in vitro or ex vivo methods that are impossible in humans and prohibitively expensive in nonhuman primates. The recent development and commercial production of positron emission tomography (PET) scanners designed for laboratory animals has now made possible novel in vivo imaging studies of small animals for a growing number of researchers. An important advantage of in vivo brain imaging studies is that measurements can be made of an individual animal at multiple time points. In addition, validation of PET measurement techniques can be readily conducted in postmortem studies. Further, the same PET methodologies that are developed and assessed in small animals can be readily extended to human studies, accelerating the transition of new discoveries from animal research to human applications.

One promising application of small animal PET is the in vivo assessment of rat brain neurochemistry. Quantification in PET studies depends on the measurement of radioactivity concentrations within distinct brain structures. To accomplish this, a 2D region of interest (ROI) or a 3D volume of interest (VOI) that corresponds to that structure must be defined within the PET image volume. At present, PET

* Corresponding author. David Geffen School of Medicine, University of California, Los Angeles, 10833 Le Conte Ave., CHS 28-117, Los Angeles, CA 90095, USA. Fax: +1-310-825-2397.
*E-mail address:* wmelega@mednet.ucla.edu (W.P. Melega).

1053-8119/$ – see front matter © 2003 Elsevier Inc. All rights reserved.
doi:10.1016/j.neuroimage.2003.07.011

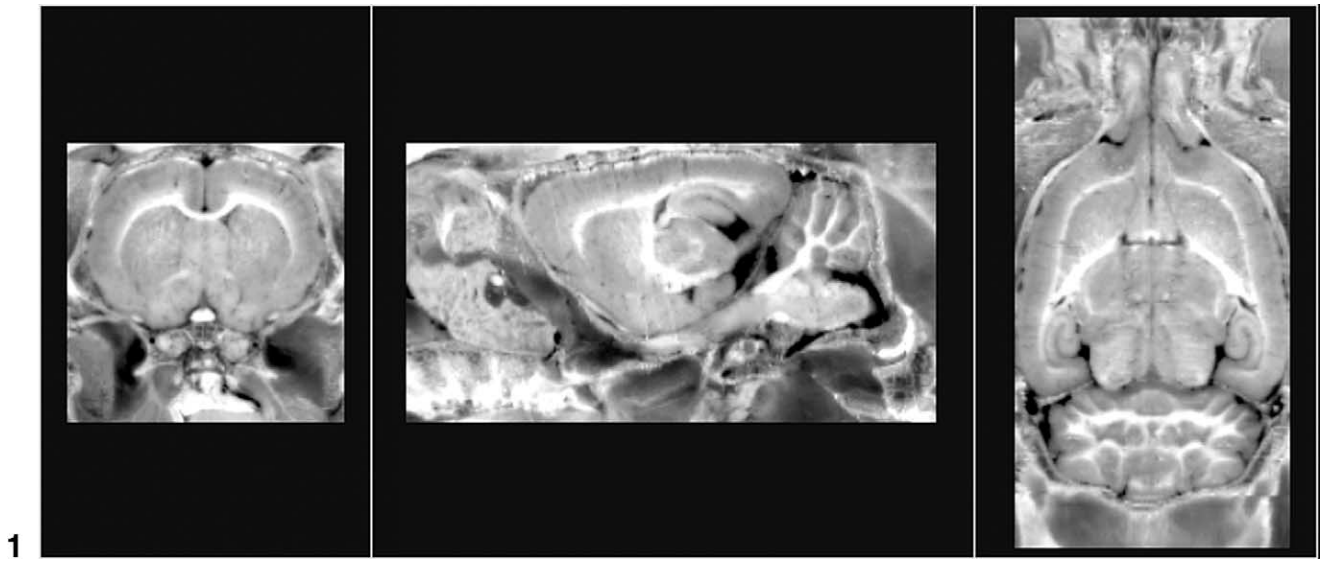


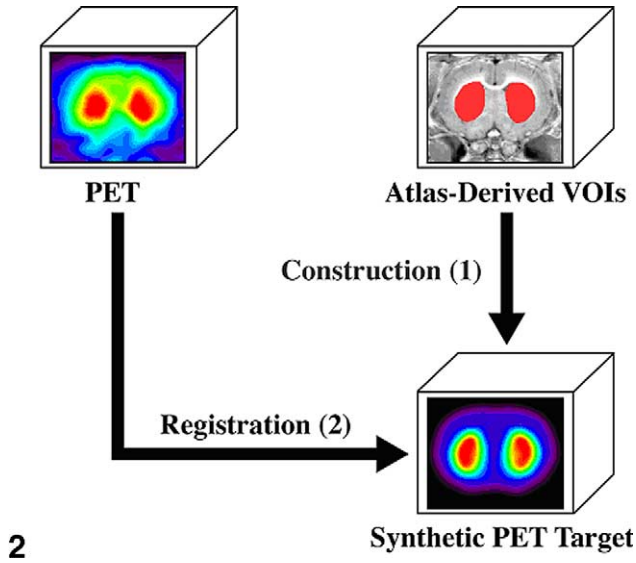


Fig. 1. VOIs were defined on a three-dimensional digital map of the rat brain. Representative coronal (left), sagittal (center), and horizontal (right) slices are displayed.

Fig. 2. The synthetic PET target method for registration of PET studies and the atlas-derived VOIs is illustrated. (1) A synthetic PET target is constructed from the atlas-derived VOIs to match the expected radiotracer distribution and spatial resolution of PET studies. (2) The PET study is then registered to the synthetic PET target. This places the PET study in alignment with the atlas-derived VOIs.

studies of the rat brain are most commonly analyzed with ROIs drawn manually on an individual plane of the PET image volume, but this method has many disadvantages. For example, the ROIs are based on the observed radioactivity distribution, and are without anatomical reference. Moreover, changes in the appearance of PET image slices, caused by various factors related to PET imaging (e.g., changes in radiotracer distribution, statistical noise, and blood flow), can result in inconsistent delineation of regional boundaries with this method, thereby leading to less accurate measurements. Further, manual drawing of ROIs is time consuming, and becomes problematic when the biological activity within the structure of interest has been altered such that the corresponding structural boundaries are not delineated by the radioactivity concentration within the structure relative to surrounding regions. Lastly, if the structure of interest covers multiple planes of the PET image volume, single-plane ROIs will not cover the entire brain structure, resulting in increased statistical noise in the measurement of radioactivity concentration within the ROI.

Alternatively, anatomical information can be used for the definition of regional boundaries in PET studies, making possible the definition of VOIs for structures that are not visually identifiable in PET image slices. Further, the drawing of VOIs that fully contain complex 3D brain structures is facilitated, maximizing the signal-to-noise ratio of mea-

surements. Such VOIs also eliminate the potential bias in measurements due to the arbitrary selection of a single plane from the PET image volume for manual ROI analysis.

In PET studies of humans and nonhuman primates, individual variability in brain anatomy necessitates use of an anatomical reference that is unique to the individual. As a result, techniques that register PET studies with a corresponding anatomical image volume obtained by magnetic resonance imaging (MRI) have been successfully developed for studies of humans and nonhuman primates (e.g., Pelizzari et al., 1989; Woods et al., 1993). One published method used a similar approach to define regional boundaries of brain structures for rat brain PET studies (Hayakawa et al., 2000). This method was based on the registration of PET and MRI image volumes, using a modified version of a method originally designed for human PET-MRI image registration (Ardekani et al., 1995). However, this method frequently required additional manual manipulation to achieve accurate registration. In general, methods for rat brain image analysis that depend on PET-MRI registration have several disadvantages. For example, the detection of regional boundaries in the rat brain with MRI requires long scan times, and the region outside the brain in the MRI often must be manually masked prior to registration. As with ROIs drawn manually on slices of PET image volumes, the definition of VOIs on individual MRI image volumes is time consuming. Further, for its widespread applicability, such an MRI-based method would require the availability of a small animal MRI scanner and an additional scan for each individual animal.

Another approach for the placement of anatomically based VOIs that has been developed for human studies is to map PET studies onto a single brain atlas (e.g., Schaltenbrand and Wahren, 1977; Talairach and Tournoux, 1988). Unlike methods that require an anatomical image of each individual animal, atlas-derived VOIs can be obtained without an additional scanning procedure. Also, consistency of VOI definition is improved because the atlas-derived VOI need be carefully defined only once. Different researchers can then use the same VOI template, thereby reducing variability in PET measurements across studies and different PET centers. The primary drawback of this method is that complex warping techniques (e.g., Bohm et al., 1986; Minoshima et al., 1994) are required for registration of human PET studies to the atlas, due to the large differences in brain anatomy between individuals (Thompson et al., 2000). In contrast, brains of rats are very similar anatomically for a given weight range, even for different strains and sex (Paxinos et al., 1985). Thus, a single brain atlas can be used for a wide range of applications that require subregional localization accuracy, e.g., determination of coordinates for stereotaxic surgical procedures (Paxinos et al., 1985). Similarly, for PET studies that use rats within a particular size and weight range (250–400 g), VOIs defined on one rat brain atlas could be used to provide excellent definition of anatomical structures. Then, for PET applications, image volumes could be mapped onto the atlas without the need for complex warping techniques.

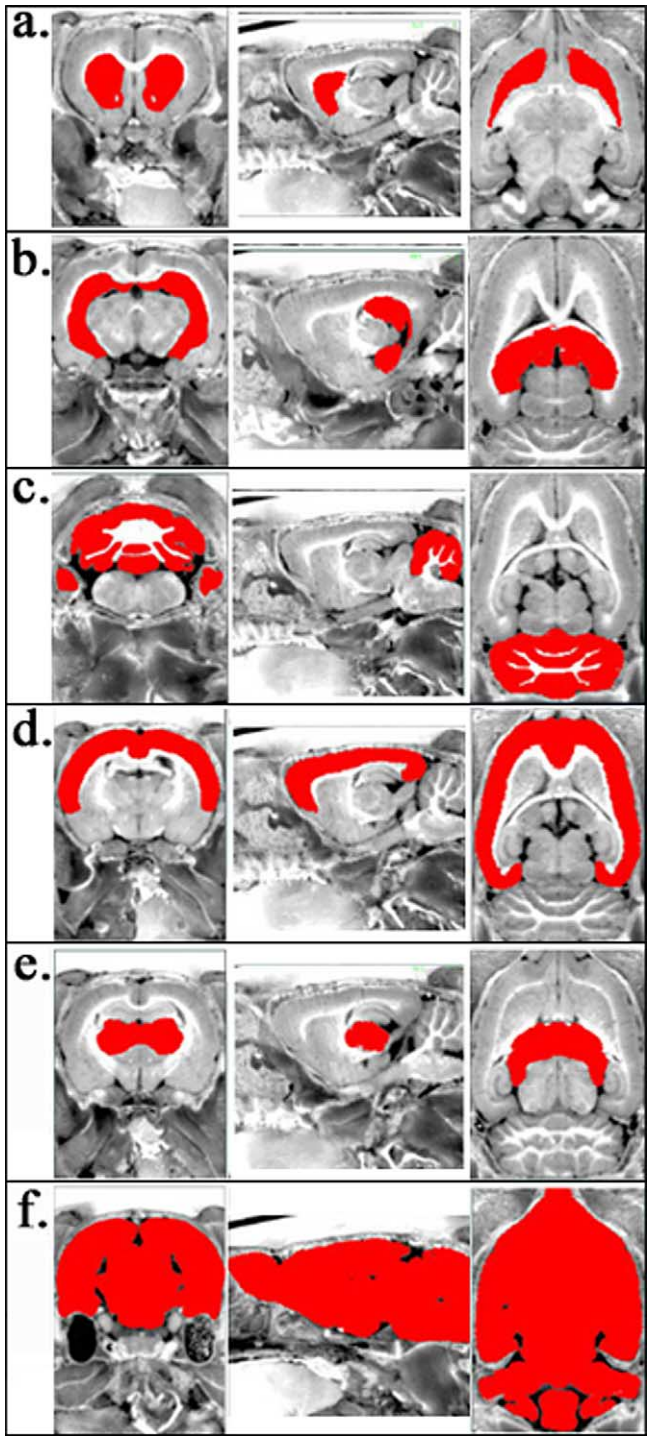


Fig. 3. Each atlas-derived VOI (red) is shown superimposed on coronal (left), sagittal (center), and horizontal (right) slices of the rat brain atlas: (a) striatum, (b) hippocampus, (c) cerebellum, (d) cerebral cortex, (e) thalamus, and (f) whole brain.

We have designed and evaluated an automated method for placement of rat brain atlas-derived VOIs onto PET studies. This method will be applicable to any image vol-

ume [generated by PET, single photon emission computed tomography (SPECT), or MRI] of a rat brain not anatomically altered by an intervention. Further, the method does not require any additional procedures (e.g., placement of fiducial markers, surgical procedures, or additional scanning procedures) at the time of the PET scanning procedure. For the present study, this method was applied to the analysis of radiotracer binding from PET studies that assessed parameters of the striatal dopamine and hippocampal serotonin systems, across different experimental conditions and in multiple animals.

## 2. Materials and methods

### *2.1. Definition of VOIs from an anatomical atlas of the rat brain*

A digital map of the Sprague-Dawley rat brain (Toga et al., 1995), constructed by cryosectioning [voxel size = $(62.5\ \mu m)^3$], was used for VOI definition (Fig. 1) (dataset provided by Arthur Toga, Laboratory of Neuroimaging, UCLA). VOIs were drawn on these images using a specialized software package (Display, Montreal Neurological Institute) that allowed the entire dataset to be visualized in three orthogonal dimensions. Each region was primarily drawn on coronal slices, with sagittal and horizontal slices used to confirm regional boundaries. The brain covered 472 coronal slices of the dataset. Published rat brain atlases were used to identify regional boundaries (Paxinos and Watson, 1986; Swanson, 1992).

The weight of the rat used in this atlas was 320 g, within the range most commonly used for PET studies (250–400 g). An advantage of this dataset is that it was obtained by cryosectioning the entire head region, in which the brain remained within the skull, preserving its structural integrity. Also, tissues outside the brain (e.g., harderian glands, salivary glands, jaw muscle, and so on) were included in the images, facilitating identification of nonbrain regions in which PET radiotracers can accumulate.

VOIs were defined for striatum, hippocampus, cerebellum, cerebral cortex, thalamus, and whole brain. A brief description of the anatomical guidelines used to define these regions is given below.

#### *2.1.1. Striatal VOI*

The striatal VOI contained the gray matter of the caudate-putamen and nucleus accumbens. Where possible, white matter, such as the anterior commissure, was excluded from the VOI. The VOI was bordered on its superior and lateral sides by the external capsule, and on its medial side by the lateral ventricle. The globus pallidus was excluded from this VOI. The left striatum and right striatum were each defined separately.

#### *2.1.2. Hippocampal VOI*

The hippocampal VOI contained the gray matter of the hippocampus. The VOI was bordered on its superior and lateral sides by the external capsule, while on its medial side, portions bordered either the ventricle or midbrain area. The left hippocampus and right hippocampus were each defined separately.

#### *2.1.3. Cerebellar VOI*

The cerebellar VOI contained the entire gray matter of the cerebellum. The fastigial nucleus, the interposed nucleus, and the dentate nucleus were excluded from this VOI.

#### *2.1.4. Cerebral cortex VOI*

The cerebral cortex VOI contained the gray matter of the cortex superior to the rhinal fissure. The area inferior to the rhinal fissure was not used because it contains small structures that are not considered part of the cortex (Paxinos and Watson, 1986; Swanson, 1992) and could not be readily excluded from the VOI. The boundaries of the VOI were defined by the skull and the external capsule.

#### *2.1.5. Thalamic VOI*

The thalamic VOI contained the thalamus proper as well as adjacent nuclei, such as the habenula and intralaminar nuclei.

#### *2.1.6. Whole brain VOI*

The whole brain VOI contained all gray and white matter within the cerebral hemisphere and brainstem. Fiber tracts such as the optic tracts that extended from the brain were excluded. Wherever visible in anatomical images, ventricles were excluded from the VOI. The outer boundaries of this VOI were matched with those outlined for the cerebral cortex and cerebellar VOIs.

### *2.2. PET Studies*

#### *2.2.1. PET scanning procedure*

Animal care and procedures were in accordance with the *Guide for Care and Use of Laboratory Animals* (National Institutes of Health Publication 865-23, Bethesda, MD) and were approved by the UCLA Chancellor's Committee for Animal Research.

The evaluation of this analysis method used data from PET studies of the rat brain that were conducted for other research studies. Data were collected on the prototype microPET system developed at UCLA, a dedicated small animal PET scanner with a 11.25-cm transaxial and 1.8-cm axial field of view (Cherry et al., 1997). Male Sprague-Dawley rats (weight range 250–400 g) were anesthesized with either an i.p. injection of a combination of 80 mg/kg ketamine and 20 mg/kg xylazine, or with 2–3% isoflurane. Animals were positioned in a stereotactic frame to ensure reproducible positioning within the microPET scanner (Rubins et al., 2001).

Studies of the striatal dopamine system were obtained using the dopamine transporter radioligand [$^{11}$C]WIN 35,428 (WIN) (Brownell et al., 1996; Wilson et al., 1996) and the $D_2$ antagonist radioligand [$^{11}$C]Raclopride (RAC) (Farde et al., 1986). The synthesis of these PET radiotracers was performed as described previously (Bauer and Wagner, 1994; Melega et al., 2000). For PET studies, approximately 37 MBq (1 mCi) of WIN or RAC was injected via the tail vein, and data were acquired dynamically for the following 30 min. Throughout data acquisition, the scanner bed was moved axially between two bed positions (0–8 min: 1 min per bed position, 9–20 min: 2 min per bed position, 21–30 min: 5 min per bed position) so that both the striatum and the cerebellum were contained within the field of view.

Control animals ($n = 4$) were each scanned twice with WIN. Other control animals ($n = 3$) were scanned once with RAC, with one animal scanned twice. In a separate study, animals ($n = 4$) received an intracerebral injection of 6-hydroxydopamine (6-OHDA) to induce a unilateral substantia nigra lesion, as previously described (Nikolaus et al., 2003). This lesion resulted in a significant reduction of WIN binding in the ipsilateral striatum (Cicchetti et al., 2002). These animals were evaluated to assess the performance of the image analysis method when reductions in WIN binding in striatum were such that the structure could not be accurately delineated by radioactivity concentration. These animals were scanned once each with WIN and RAC.

Studies of the hippocampal serotonin system were obtained using the 5-$HT_{1A}$ antagonist radioligand 4-(2′-methoxyphenyl)-1-[2′-(*N*-2′-pyridinyl)-*p*-[$^{18}$F]fluoro-benzamido] ethylpiperazine (MPPF) (Plenevaux et al., 2000). The synthesis of MPPF was performed as described previously (Plenevaux et al., 2000). For PET studies, approximately 37 MBq (1 mCi) of MPPF was injected via the tail vein, and data were dynamically acquired for the following 35 min. Control animals ($n = 4$) were scanned under ketamine-xylazine (80–20 mg/kg) anesthesia. These studies were repeated 1 week later under isoflurane (2–3%) anesthesia.

#### 2.2.2. PET image reconstruction

PET studies were reconstructed using a statistical maximum a posteriori probability algorithm (MAP) (Qi et al., 1998), which has been shown to result in improved spatial resolution and noise properties in microPET images compared to filtered backprojection (Chatziioannou et al., 2000). MAP reconstructions included calculated attenuation correction (Siegel and Dahlbom, 1992), and were performed with the following reconstruction parameters: pixel size = 0.5 mm, $\beta$ (smoothing parameter) = 1.0. The resulting image volumes contained 24 image planes, with a slice thickness of 0.75 mm, and the $\beta$ value selected resulted in a volumetric spatial resolution of approximately 1.5 mm (Chatziioannou et al., 2000). Data summed over the entire scan time were used for image reconstruction. This was done to minimize statistical noise in resultant image volumes for the purpose of registration.

### 2.3. Registration of PET studies and atlas-derived VOIs

#### 2.3.1. Automated methods for image registration

For VOI placement, PET studies were registered to the VOI template with an automated image registration algorithm. Registration was accomplished as a rigid body transformation, with no warping or scaling. Two of the most widely used automated image registration algorithms were evaluated for this purpose: mutual information (MI) (Wells et al., 1996) and automated image registration (AIR) (Woods et al., 1992).

The MI algorithm is an iterative technique that determines the best alignment of two image volumes by finding the orientation for which the voxel values of the two image volumes are maximally dependent. MI has been shown to be successful for both intra- and intermodality image registration in humans and nonhuman primates (Wells et al., 1996; Maes et al., 1997; Studholme et al., 1997), but has not been previously evaluated for registration of rat brain images. For this work, MI registrations were accomplished using software called Rview, provided by Dr. Colin Studholme at UCSF.

The AIR algorithm is also an iterative technique that was designed based on the theory that the voxel values in accurately aligned image volumes are related by a single multiplicative factor and that, therefore, the position for which the variance of the ratio between corresponding voxel values is minimized is the best alignment of the two image volumes. AIR has also been validated for intra- and intermodality registration for human and nonhuman primate images (Woods et al., 1992, 1993, 1998a,b), but has not been evaluated for registration of rat brain images. For this work, AIR registrations were accomplished using software (AIR 3.08) obtained from the Laboratory of Neuroimaging at UCLA.

#### 2.3.2. Synthetic PET target technique

To optimize the registration of PET studies and the VOI template, a synthetic PET image volume is first generated from the atlas-derived VOIs to serve as a target for registration. This method is illustrated in Fig. 2. A unique synthetic PET target is constructed for each type of PET study to be analyzed. To make the synthetic PET target as similar as possible to corresponding PET studies, values are assigned to the voxels in each VOI corresponding to the expected radioactivity concentration within that brain structure. The synthetic PET target image volume is then blurred to match the spatial resolution of the PET scanner. The resultant synthetic PET target should closely match corresponding PET studies in the size, shape, and relative voxel values of brain structures, and thus be optimal for use in MI and AIR registrations. The sensitivity of registration to the voxel values used to construct the synthetic PET target was also investigated (see Section 2.4).

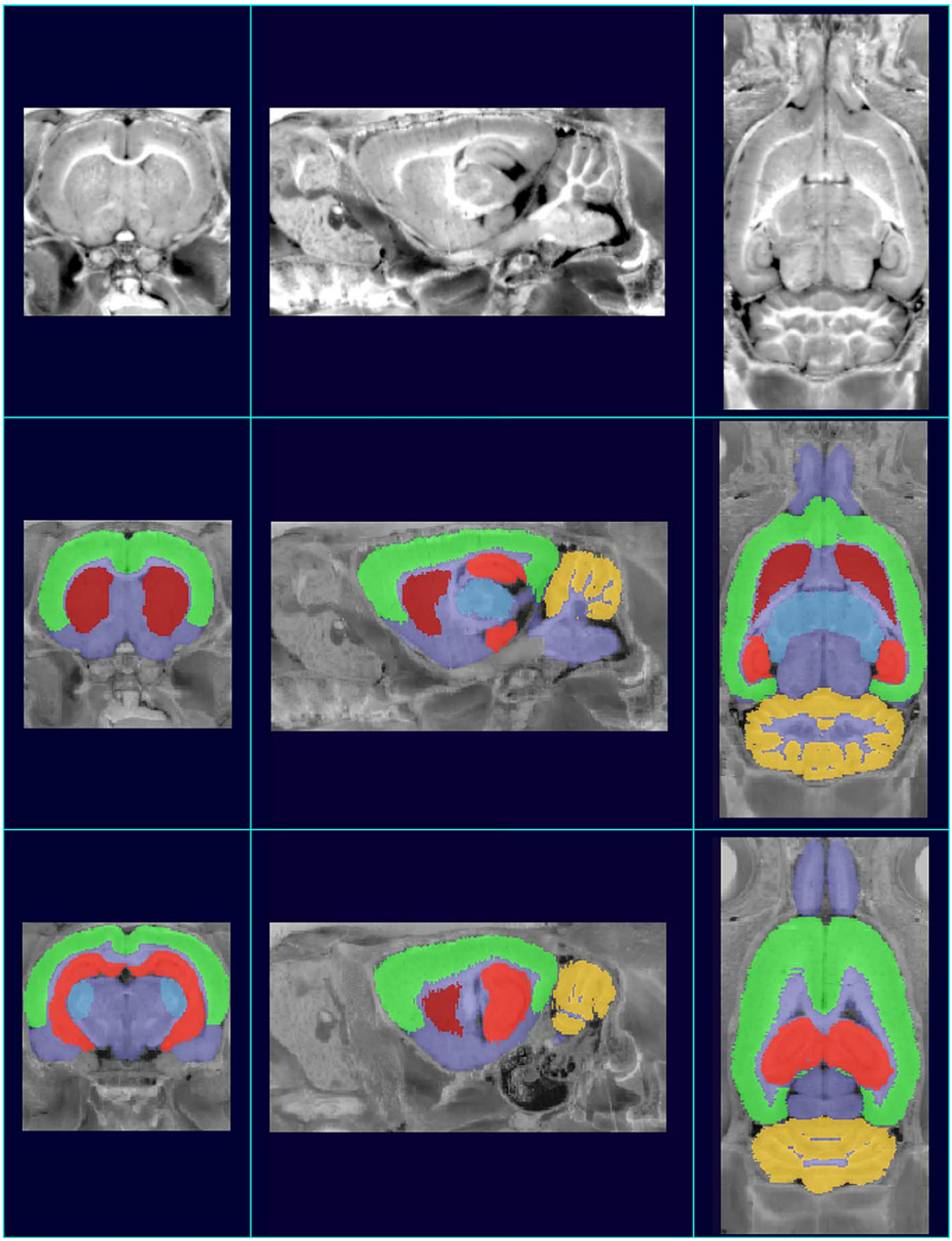

Fig. 4. The atlas-derived VOIs are shown superimposed on coronal (left), sagittal (center), and horizontal (right) slices of the rat brain atlas (shown in top row without VOIs), demonstrating the relative positions of the VOIs. VOIs: striatum (red), hippocampus (orange), cerebral cortex (green), cerebellum (yellow), thalamus (blue), and whole brain (purple).

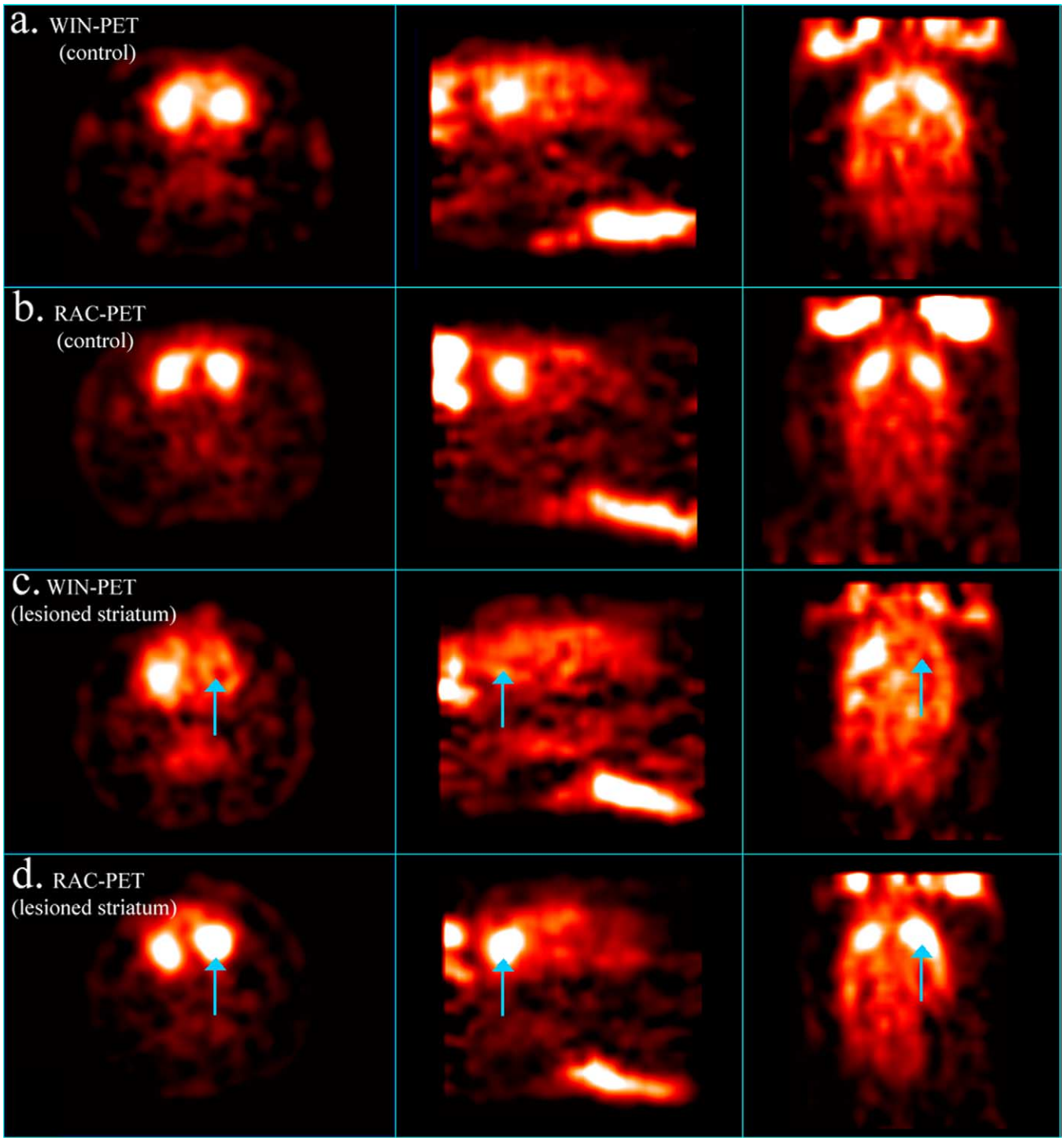


Fig. 5. Coronal (left), sagittal (center), and horizontal (right) image slices from representative WIN- and RAC-PET studies are displayed: (a) WIN, control subject, (b) RAC, control subject, (c) WIN, nigrostriatal lesion subject, and (d) RAC, nigrostriatal lesion subject. Arrows point to lesioned striatum.

### *2.4. Evaluation experiments*

#### *2.4.1. Initial evaluation of AIR and MI with PET studies of the rat brain*

The performance of the two automated registration algorithms, AIR and MI, for registering PET studies of the rat brain was evaluated. The image volume from a WIN-PET study of a control animal received the following software transformations: translations of 0.4, 1.2, 2, 4, and 8 mm in the axial and transaxial directions, and rotation by 2, 4, 8, 16, and 32 degrees in all three directions. Each resultant image volume was then registered with the original image volume by both AIR and MI. For each registration attempt, the transformation and rotation error was determined.

Table 1
Voxel values assigned to synthetic PET targets and resultant registration failures for WIN and RAC[a]

| Synthetic PET target | Assigned Voxel value: striatum | Assigned voxel value: brain (non-striatum) | Obvious registration failures (of 20 PET studies) |
|---|---|---|---|
| WIN1 | 255 | 0 | 8 |
| WIN2 | 255 | 150 | 0 |
| WIN3 | 255 | 100 | 0 |
| WIN4 | 255 | 200 | 0 |

[a] All voxels outside of the brain were assigned a value of zero.

### 2.4.2. Evaluation of registration of PET studies and synthetic PET targets

A set of synthetic PET targets was constructed for WIN- and RAC-PET studies, and another set was constructed for MPPF-PET studies. The voxel values assigned to each synthetic PET target (WIN1-WIN4, MPPF1-MPPF6) are listed in Tables 1 and 2. Synthetic PET targets were not altered for use with PET studies of unilateral nigrostriatal lesion animals. After assignment of voxel values, each synthetic PET target was smoothed by boxcar averaging of a width of 1.5 mm, to match the spatial resolution of microPET images reconstructed with MAP (Chatziioannou et al., 2000).

PET studies were registered with each corresponding synthetic PET target using the MI procedure. WIN- and RAC-PET studies of unilateral nigrostriatal lesion animals were registered to the same set of synthetic PET targets as those of control animals. As with any automated image registration algorithm, it was necessary for the user to check for obvious registration failures. These were counted for each synthetic PET target. Each PET study of a given radiotracer underwent the same processing before registration, including a spatial transformation to place the PET study in closer alignment with the synthetic PET target as a starting point for registration.

The objective of this evaluation was to find a single synthetic PET target that would result in registration to the atlas-derived VOI template of all PET studies obtained with a given radiotracer, with no obvious registration failures.

### 2.4.3. Evaluation of synthetic PET target smoothing and initial position range

Experiments were performed to assess the effects of two factors on the accuracy of registrations performed in the previous section, namely the amount of synthetic PET target smoothing and the initial position of the PET study relative to the synthetic PET target prior to registration.

First, the dependence of registration on the smoothing factor applied to the synthetic PET target was investigated. Additional copies of the synthetic PET targets MPPF3 and WIN2 (Tables 1 and 2) were constructed that were smoothed with boxcar averaging widths of 1.0, 2.0, and 2.5 mm. These synthetic PET targets were then evaluated in the same manner as those described in the previous section.

Next, the range of initial positions of the PET study, relative to the synthetic PET target, that would result in successful registration was determined. Starting with the PET study aligned with the synthetic PET target, the position of the PET study was translated by increments of 0.5 mm prior to each attempt at registration until an obvious registration failure occurred. This procedure was carried out in both directions along all three orthogonal axes. Included in this evaluation were selected WIN- and RAC-PET studies (of control and unilateral nigrostriatal lesion animals) registered to the synthetic PET targets WIN2 and WIN3 (Table 1), and MPPF-PET studies registered to the synthetic PET targets MPPF3 and MPPF5 (Table 2).

### 2.4.4. Comparison with maximum radioactivity concentration measurement

The following evaluation was performed to demonstrate that once a PET study is registered to a synthetic PET target without an obvious registration error, resultant radioactivity concentration measurements will not be in error due to misalignment of brain structures in the PET study and corresponding VOIs. Following each MI registration, the orientation of the PET study relative to the atlas-derived

Table 2
Voxel values assigned to synthetic PET targets and resultant registration failures for MPPF[a]

| Synthetic PET target | Assigned voxel value: hippocampus | Assigned voxel value: brain (non-hippocampus) | Obvious registration failures (of 8 PET studies) |
|---|---|---|---|
| MPPF1 | 255 | 0 | 2 |
| MPPF2 | 150 | 0 | 2 |
| MPPF3 | 255 | 150 | 0 |
| MPPF4 | 255 | 100 (cerebral cortex 175) | 2 |
| MPPF5 | 255 | 100 | 0 |
| MPPF6 | 255 | 200 | 1 |

[a] All voxels outside of the brain were assigned a value of zero.

VOIs was varied to find the highest possible radioactivity concentration measurement (average voxel value within the VOI) for the structure of highest radioactivity concentration in the PET study (striatum for WIN- and RAC-PET studies; hippocampus for MPPF-PET studies). It was expected that, for localized radiotracer uptake in small structures, the measured radioactivity concentration for this structure would be maximized at the point of best registration of the structure and its VOI. The position of maximum radioactivity concentration measurement for this structure was determined by a program written in Interactive Data Language (Research Systems Inc., Denver, CO), using the Powell procedure, which minimizes a function of multiple independent variables (Press et al., 1997). Included in this evaluation were WIN- and RAC-PET studies (of control and unilateral nigrostriatal lesion animals) registered to the synthetic PET targets WIN2 and WIN3 (Table 1), and MPPF-PET studies registered to the synthetic PET targets MPPF3 and MPPF5 (Table 2).

#### *2.4.5. Comparison of atlas-derived VOIs and manually drawn ROIs*

For comparison with the atlas-derived VOI method, a template set of ROIs was manually drawn and applied to all PET studies of control animals. These ROIs were drawn and placed by one of the authors, who had extensive experience in manual ROI definition and who was blinded to the results obtained using atlas-derived VOIs. ROIs were drawn on images of WIN and RAC binding for left striatum, right striatum, and cerebellum, and on images of MPPF binding for left hippocampus, right hippocampus, and cerebellum. Striatal and hippocampal ROIs were placed on the single plane (slice thickness = 0.75 mm) of highest radioactivity concentration within the PET image volume, and the cerebellar ROI was placed on a plane that was at a fixed distance from the plane of the striatal or hippocampal ROI. ROIs were aligned with the corresponding brain structure, as estimated by the radioactivity concentration observed in the PET image plane.

Measurements of radioactivity concentration obtained from these ROIs and from the atlas-derived VOIs in the same PET studies were used to calculate binding ratios [Eq. (1)] for striatum: right, left, and total (WIN- and RAC-PET studies), and for hippocampus: right, left, and total (MPPF-PET studies). Image data summed over the entire PET scanning procedure were used for this calculation. Included in this evaluation were WIN- and RAC-PET studies registered to the synthetic PET targets WIN2 and WIN3 (Table 1), and MPPF-PET studies registered to the synthetic PET targets MPPF3 and MPPF5 (Table 2).

$$\text{Binding Ratio} = \left(\frac{Specific\ Binding}{Nonspecific\ Binding}\right) = \left(\frac{Tissue - Cerebellum}{Cerebellum}\right) \quad (1)$$

The relative accuracy of the two sets of binding ratio measurements was then determined by two comparsions. First, a within-subject, within-scan comparison was performed. The right-left difference in the binding ratio for the designated structure was determined for each PET study, and the average of these differences was calculated across PET studies obtained with each radiotracer. The method that yielded the lower average right-left difference was considered to be more accurate, based on the assumption that no major asymmetry in WIN, RAC, or MPPF binding values should be observed in control animals. Results from previous in vitro studies in control animals support these assumptions. For example, similar values for right and left striatal dopamine concentration levels have been measured by high performance liquid chromatography (HPLC) (Cohen et al., 2003). Likewise, similar values for right and left hippocampal 5-$HT_{1A}$ density levels have been measured by autoradiography (Ait Amara et al., 2001).

Next, the reproducibility of repeat measures of binding ratio in the same animal determined was compared for the two methods. The binding ratio for the total striatum was determined for each WIN-PET study, and for each pair of studies of the same animal, the difference divided by the mean of the two measured binding ratios was calculated.

## 3. Results

### *3.1. Definition of VOIs from an anatomical atlas of the rat brain*

VOIs were defined for the rat brain striatum, hippocampus, cerebellum, cerebral cortex, thalamus, and whole brain. These VOIs are displayed in Figs. 3 and 4. The volume of each VOI is shown in Table 3. The volume of brain structures (range 0.045–2.045 $cm^3$) far exceeds the approximate microPET resolution with MAP reconstruction (~0.003 $cm^3$), demonstrating that these brain structures are large enough to analyze with the microPET system. With further improvement of the spatial resolution of PET, VOIs can be defined in a similar fashion for smaller brain structures.

Table 3
Volumes of rat brain VOIs

| Atlas-derived VOI | Volume |
|---|---|
| Left striatum | 0.045 $cm^3$ |
| Right striatum | 0.045 $cm^3$ |
| Left hippocampus | 0.051 $cm^3$ |
| Right hippocampus | 0.053 $cm^3$ |
| Cerebellum | 0.247 $cm^3$ |
| Cerebral cortex | 0.546 $cm^3$ |
| Thalamus region | 0.065 $cm^3$ |
| Whole brain | 2.045 $cm^3$ |
| MicroPET resolution (MAP reconstruction, approx.) | $(1.5\ mm)^3 = (0.15\ cm)^3 = 0.0034\ cm^3$ |

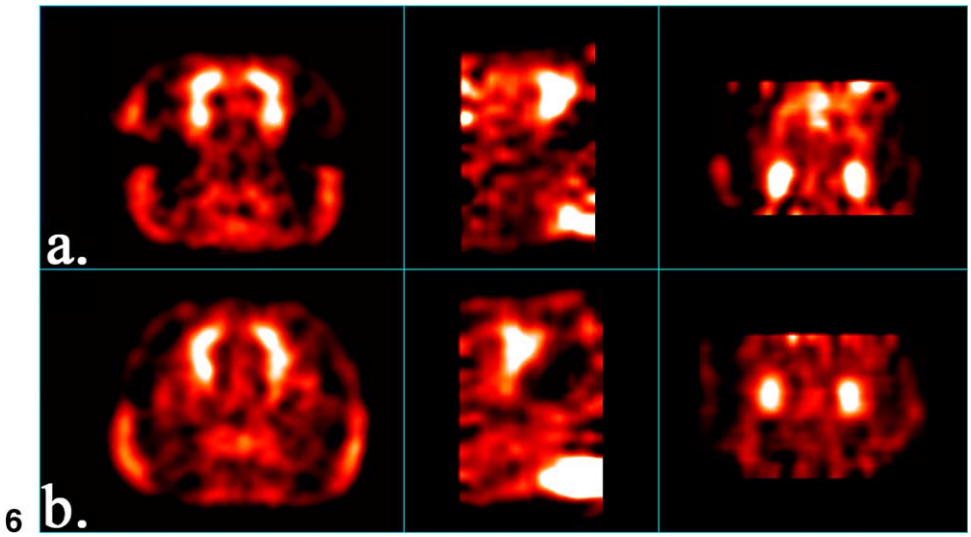


6

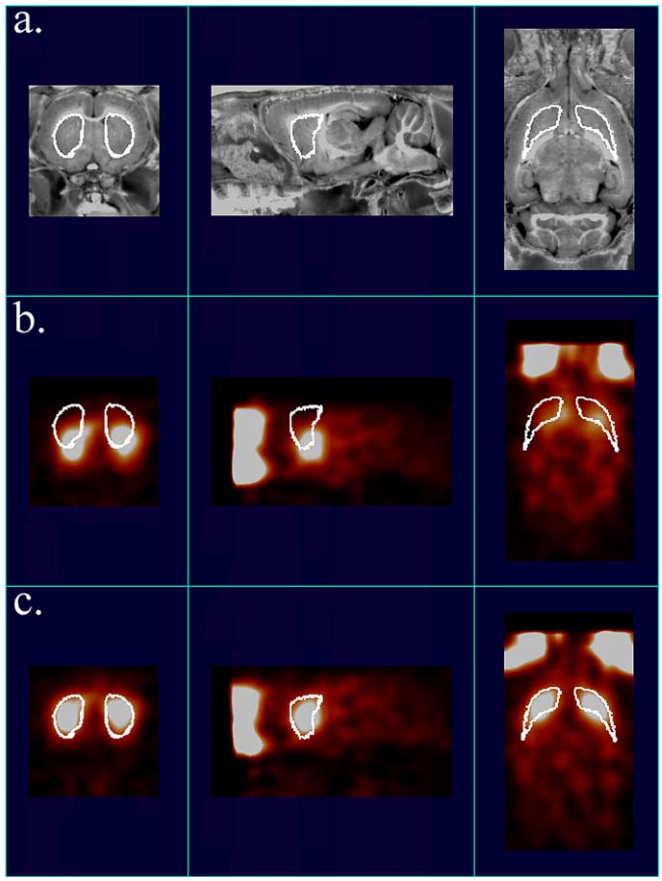


7

Fig. 6. Coronal (left), sagittal (center), and horizontal (right) image slices from two representative MPPF-PET studies are displayed.
Fig. 7. The outline of the striatal VOI is shown superimposed on coronal (left), sagittal (center), and horizontal (right) slices of (a) the rat brain atlas, (b) a PET study prior to registration, and (c) the same PET study following registration to the synthetic PET target. This registration procedure results in the alignment of the PET study and the VOI template.

### *3.2. PET studies*

Twenty-four PET studies of 15 subjects were obtained for this evaluation. Image slices from representative WIN- and RAC-PET studies are displayed in Fig. 5. In all WIN- and RAC-PET studies, the brain was delineated in image slices by its greater radioactivity concentration relative to surrounding tissues. Also, in studies of control animals, the left striatum and right striatum were each similarly delineated within the brain. In animals with a unilateral nigro-

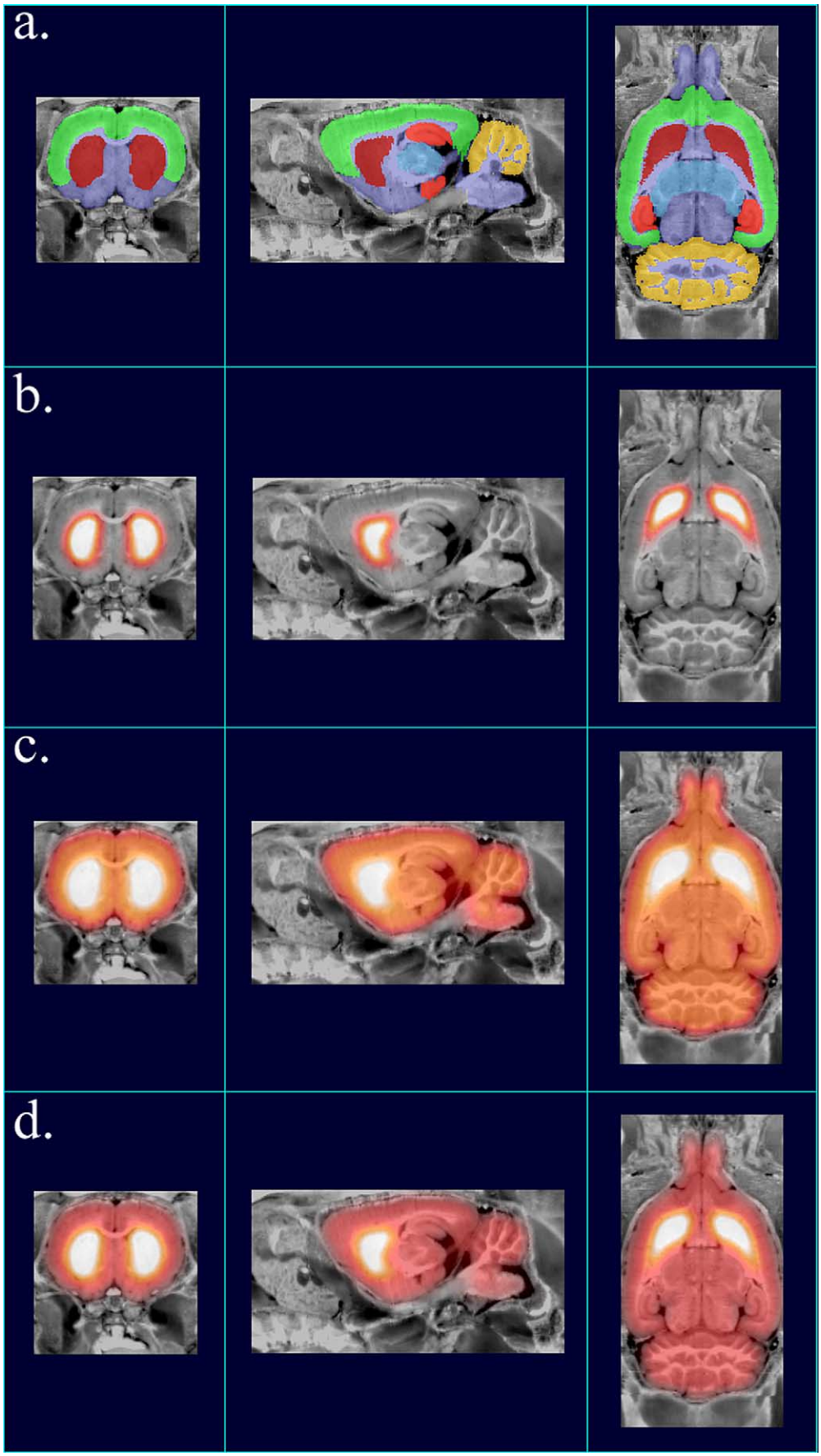


Fig. 8. The atlas-derived VOIs and three synthetic PET targets for WIN- and RAC-PET studies are shown superimposed on coronal (left), sagittal (center), and horizontal (right) slices of the rat brain atlas: (a) atlas-derived VOI template, (b) WIN1, (c) WIN2, and (d) WIN3. The voxel values assigned to each synthetic PET target are listed in Table 1.

striatal dopamine lesion induced by 6-OHDA ($n = 4$), radioactivity concentration in the ipsilateral striatum was markedly reduced in WIN-PET studies, such that the structure was no longer delineated in image slices. In two of those four animals, an increase in radioactivity concentration in the ipsilateral striatum was observed in image slices of RAC-PET studies.

Image slices from representative MPPF-PET studies are displayed in Fig. 6. In these PET studies, the left hippocampus and right hippocampus were each delineated in image slices by their greater radioactivity concentration relative to surrounding brain structures. As the radioactivity concentration within other brain regions was comparable to surrounding nonbrain tissues in these PET studies, the brain was not similarly delineated in image slices of MPPF-PET studies.

### *3.3. Evaluation experiments*

#### *3.3.1. Initial evaluation of AIR and MI with PET studies of the rat brain*

Registration errors were negligible when the MI procedure was used to register a translated or rotated image volume from a WIN-PET study to its original image volume. The average translation error was 0.05 mm (0.05 SD), with a maximum translation error of 0.20 mm, and the average rotation error was 0.05° (0.03 SD), with a maximum rotation error of 0.10°. The largest MI registration errors occurred following large-scale rotations (16° and 32°) of the image volume.

In comparison, AIR registration resulted in an average translation error of 0.65 mm (0.44 SD), with a maximum translation error of 1.61 mm, and an average rotation error of 1.00° (0.67 SD), with a maximum rotation error of 2.53°. No correlation between registration errors and the magnitude of the transformation applied prior to registration was observed. Since AIR has a large number of parameters that are selected by the user, it is possible that a different combination of parameter settings could have resulted in better registration accuracy. However, such a combination was not found during this study. As a result of these findings, the MI algorithm was selected for registration of PET studies and synthetic PET targets, for the placement of atlas-derived VOIs.

#### *3.3.2. Evaluation of registration of PET studies and synthetic PET targets*

Image slices from a representative PET study before and after successful registration to a synthetic PET target are shown in Fig. 7. Example synthetic PET targets are displayed in Figs. 8 and 9.

Following the MI registration procedure, all WIN- and RAC-PET studies appeared registered to every synthetic PET target except for WIN1. The complete results of these registrations are listed in Table 1, while image slices from representative WIN- and RAC-PET studies are shown superimposed on the rat brain atlas following registration with a synthetic PET target in Fig. 10. Of the synthetic PET targets without any obvious registration failures, WIN2 and WIN3 were selected for further analysis, as they were more similar in appearance to PET studies than WIN4.

Following the MI registration procedure, all MPPF-PET studies appeared registered to the synthetic PET targets MPPF3 and MPPF5, while at least one obvious registration failure occurred with each of the other synthetic PET targets. The complete results of these registrations are shown in Table 2, while image slices from representative MPPF-PET studies are shown superimposed on the rat brain atlas following registration with a target image volume in Fig. 11.

Every PET study in this evaluation was registered to more than one synthetic PET target without an obvious failure. Further, the same synthetic PET target could be used for registration of all PET studies of a given radiotracer to the atlas-derived VOI template, even those PET studies where radiotracer distribution had been altered by a unilateral nigrostriatal lesion (Fig. 10d and e).

#### *3.3.3. Evaluation of target image volume smoothing and initial position range*

When the degree of smoothing was varied for the synthetic PET target WIN2 and MPPF3, and the registration of PET studies and corresponding targets was repeated, all PET studies again appeared registered to the synthetic PET targets.

The ranges of initial placement that resulted in registration of the control WIN-PET study to its synthetic PET target ranged from 11.5 mm in the vertical direction to 20.0 mm in the medial-lateral direction. These ranges were reduced in all directions in the WIN-PET study of a unilateral nigrostriatal lesion animal compared to the corresponding study of a control animal, and the smallest range was again observed in the vertical direction (9.0 mm). The ranges of initial placement that resulted in registration of RAC-PET studies ranged from 9.0 mm in the medial-lateral direction to 18.0 mm in the axial direction. The ranges observed for the RAC-PET study of a unilateral nigrostriatal lesion animal were very similar to those for the corresponding study of a control animal. The ranges of initial displacement that resulted in registration of each MPPF-PET study to the synthetic PET ranged from 7.0 mm in the medial-lateral direction to 12.0 in the axial direction. These ranges were similar for MPPF studies using each type of anesthesia.

#### *3.3.4. Comparison with maximum radioactivity concentration measurement*

The difference between the measured radioactivity concentration (determined by MI registration of the PET study to the corresponding synthetic PET target) and the maximum possible radioactivity concentration measurement for the VOI representing the structure of highest radioactivity concentration was 2% or less for all PET studies evaluated, including PET studies of unilateral nigrostriatal lesion ani-

Table 4
Comparison of measured VOI value to maximum value

| Radiotracer | Animal[a] | Synthetic PET target | VOI value difference (average across PET studies) |
|---|---|---|---|
| WIN | Control | WIN2 | 0.7% (0.4 SD) |
| WIN | Control | WIN3 | 0.6% (0.3 SD) |
| WIN | Lesion | WIN2 | 1.1% (0.8 SD) |
| WIN | Lesion | WIN3 | 0.7% (0.3 SD) |
| RAC | Control | WIN2 | 0.6% (0.2 SD) |
| RAC | Control | WIN3 | 0.5% (0.3 SD) |
| RAC | Lesion | WIN2 | 0.5% (0.2 SD) |
| RAC | Lesion | WIN3 | 0.5% (0.3 SD) |
| MPPF | Control | MPPF3 | 0.7% (0.3 SD) |
| MPPF | Control | MPPF5 | 0.6% (0.3 SD) |

[a] Lesion = animal received a unilateral nigrostriatal lesion prior to PET study.

mals. The average difference in these values for each type of PET study is shown in Table 4. These results imply that close alignment was achieved between the designated brain structure and the corresponding VOI when obvious failure was not observed in registration of the PET study with the synthetic PET target.

### *3.3.5. Comparison of atlas-derived VOIs and manually drawn ROIs*

In control animals, the right-left differences in the binding ratio measured with atlas-derived VOIs were lower than those measured with manually drawn ROIs for all radiotracers. This difference was statistically significant ($P < 0.01$; paired, two-tailed $t$ test) for PET studies of WIN binding. These results are shown in Fig. 12. The variability of binding ratios measured from repeat PET studies of the same animals with atlas-derived VOIs was also slightly lower than the variability measured from the same PET studies with manually drawn ROIs. These results are shown in Fig. 13.

## 4. Discussion

We have designed and evaluated an automated method for placement of rat brain atlas-derived VOIs onto PET studies. The first step toward the development of this method was the definition of VOIs representing major structures of the rat brain on a set of digitized cryosectioned rat brain images. Definition of structural boundaries, while arbitrary in some image planes, generally corresponded to the 2D representation in a commonly used stereotactic rat brain atlas (Paxinos and Watson, 1986). Nonetheless, the VOIs were rigorously defined and can provide a standardized, detailed dataset that would not be possible to generate separately for each PET study to be analyzed. The next step was the development of the synthetic PET target method for alignment of PET studies and VOIs. The PET studies were registered to a synthetic PET target that was constructed from the atlas-derived VOI, and thus brought into register with the VOIs. Results of an initial experiment showed that the MI algorithm achieved better results than the AIR algorithm for the registration of rat brain PET studies. As a result, the MI algorithm was used for registration of PET studies and synthetic PET targets.

The method relies on several assumptions, and each of these was considered for evaluation. First, it is assumed that the VOIs accurately match the brain structures in the anatomical atlas on which they were defined. This is unlikely to be a significant source of error, as the anatomical images had excellent spatial resolution and boundaries of the brain structures were distinct. Another assumption is that the rat brain anatomical atlas, based on a single animal, accurately matches the anatomy of other animals. Since the brain anatomy is very similar for rats of corresponding weight, even for different sexes and strains, it can be safely assumed that intersubject variability in brain anatomy should not be a significant source of error for measurements with atlas-based VOIs. Exceptions would be rat subjects with abnormal brain anatomy, such as subjects in experiments involving brain tumors or the surgical removal of brain tissue, as well as those whose size was markedly different from the subject used for the anatomical atlas (320 g). Finally, it is assumed that PET studies can be accurately registered with synthetic PET targets for placement of atlas-derived VOIs, despite the wide variety of radiotracers used for rat brain PET studies, and even though the radiotracer distribution in PET studies is often altered by interventions such as a surgical procedures or pharmacological challenges. Registration was expected to be the most likely source of error, and was the primary focus of this evaluation. Unfortunately, there is not an obvious single experiment to conclusively validate the accuracy of this registration. Instead, a series of evaluations were performed to first assess the accuracy of registration, and then to assess the relative precision of resultant radioactivity concentration measurements compared to those obtained by manually drawn ROIs.

For the evaluation, the atlas-derived VOI method was applied to the analysis of PET studies that assessed parameters of the striatal dopamine and hippocampal serotonin systems. It was found that each evaluated PET study could be registered to more than one synthetic PET target. Further, the same synthetic PET target could be used for registration of all PET studies of the same radiotracer without obvious registration failures, even for PET studies following an intervention that resulted in an alteration of radiotracer distribution. These results showed that registration was not affected by unilateral alterations to the radiotracer distribution in PET studies, indicating that for interventions that cause only unilateral changes, the same synthetic PET target can be used for both control and experimental PET studies. Further, registration was not highly sensitive to small changes in the voxel values assigned to the synthetic PET target. However, large-scale changes in assigned voxel values did affect registration. For example, the synthetic PET

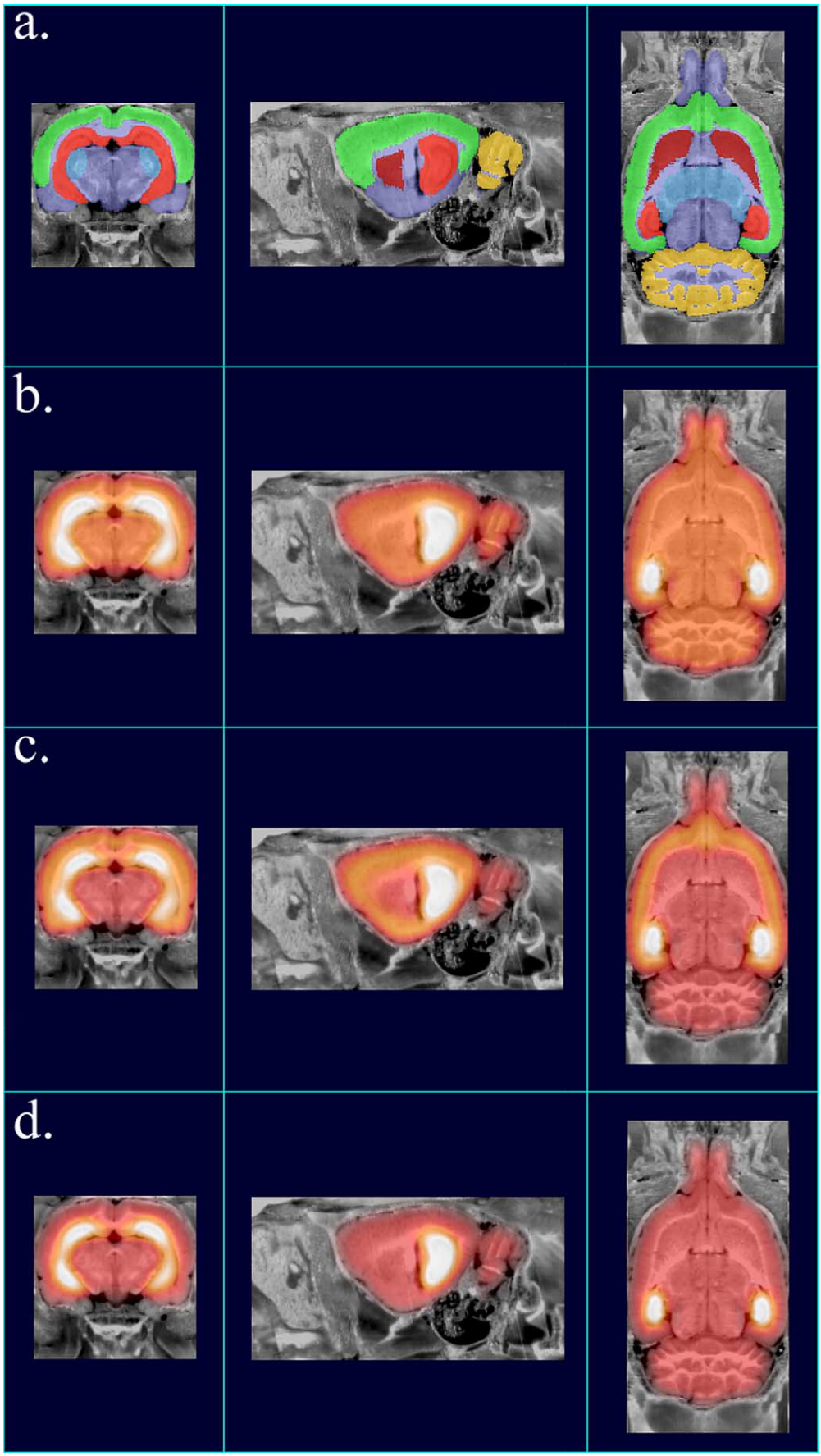


Fig. 9. The atlas-derived VOIs and three synthetic PET targets for MPPF-PET studies are shown superimposed on coronal (left), sagittal (center), and horizontal (right) slices of the rat brain atlas: (a) atlas-derived VOI template, (b) MPPF3, (c) MPPF4, and (d) MPPF5. The voxel values assigned to each synthetic PET target are listed in Table 2.

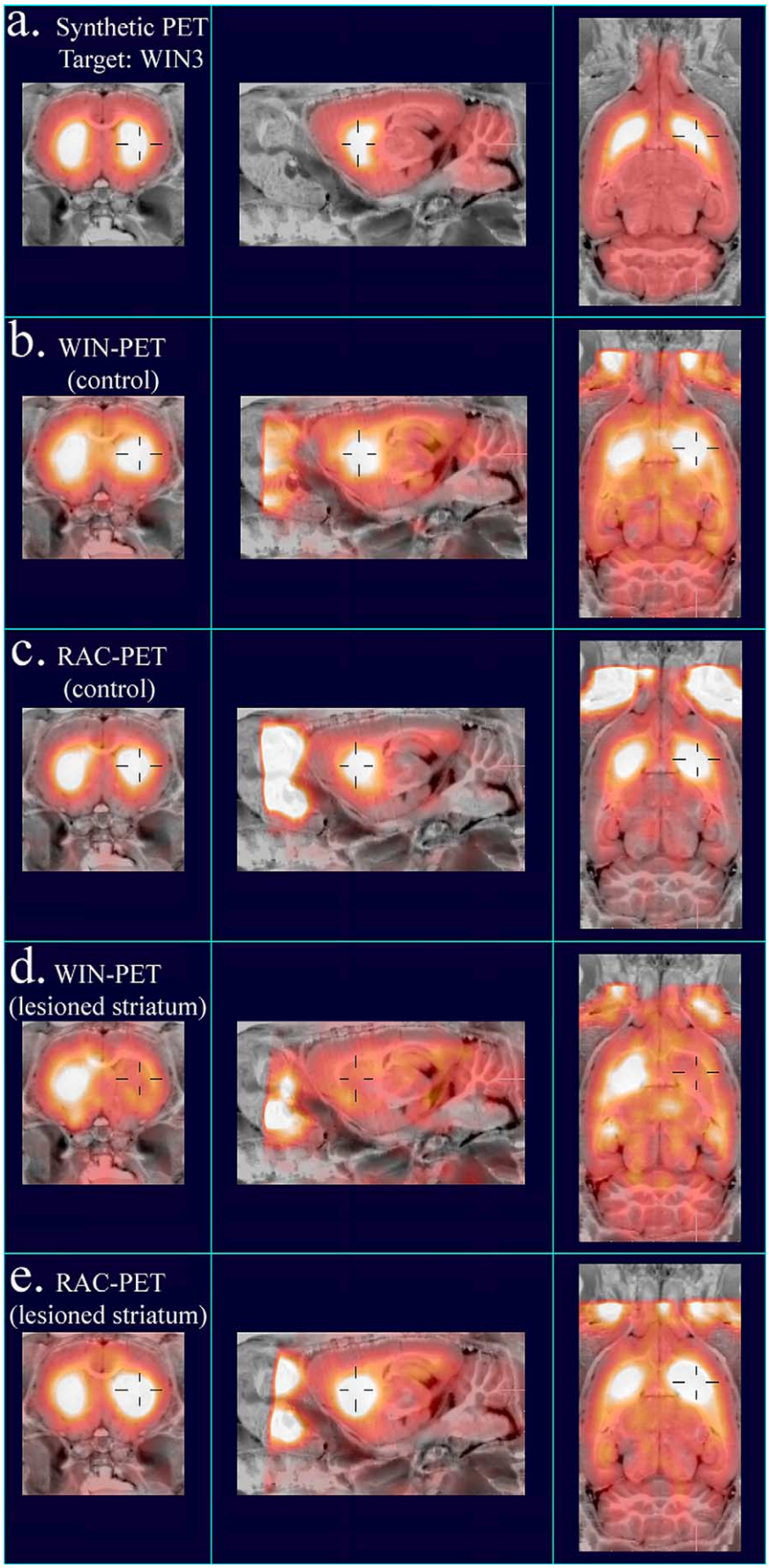


Fig. 10. Coronal (left), sagittal (center), and horizontal (right) image slices from representative WIN- and RAC-PET studies are shown superimposed on the rat brain atlas following registration with a synthetic PET target: (a) synthetic PET target WIN3, (b) WIN, control subject, (c) RAC, control subject, (d) WIN, nigrostriatal lesion subject, and (e) RAC, nigrostriatal lesion subject. The cross-hairs cover the same point on the atlas in all images.

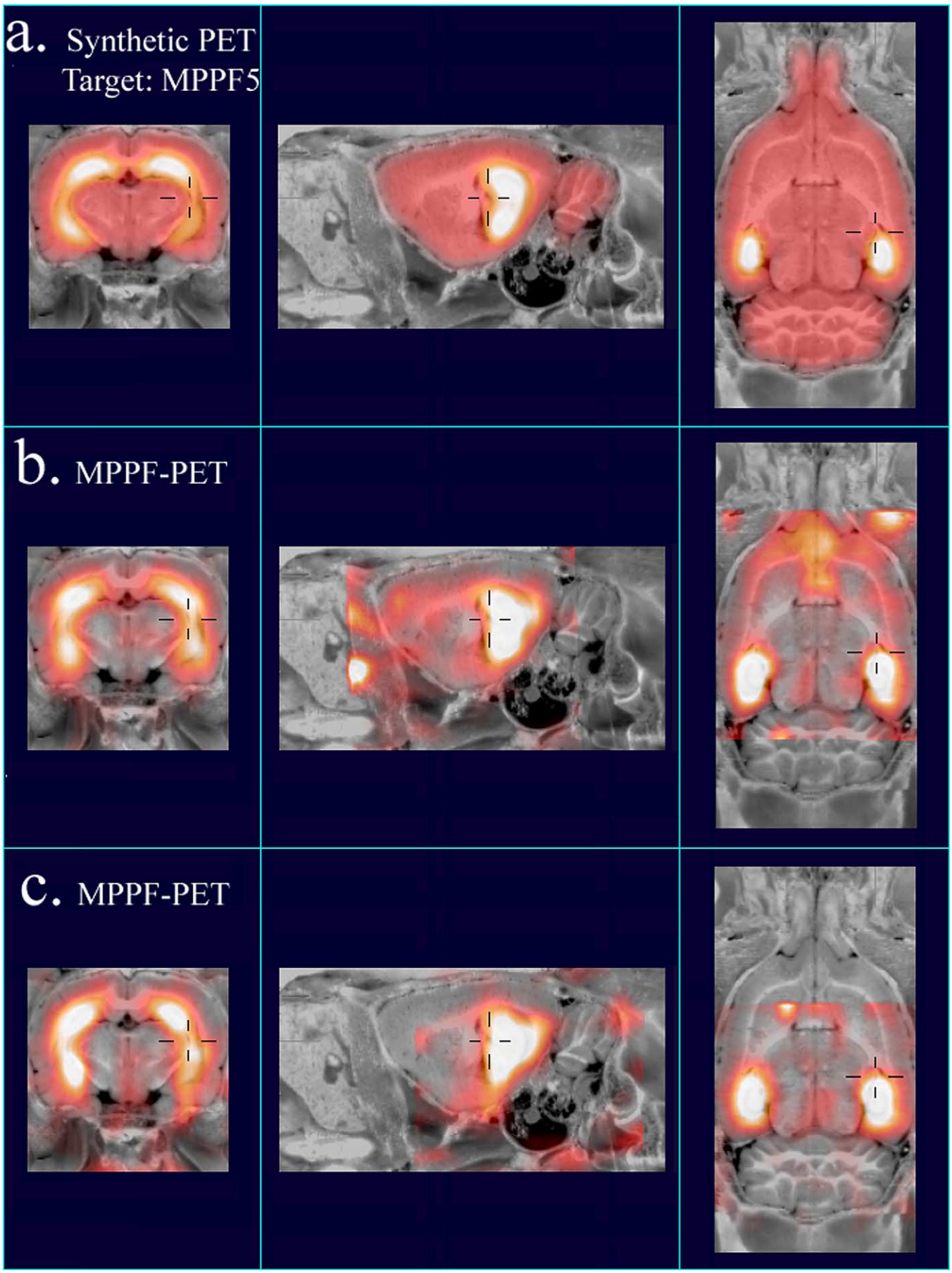


Fig. 11. Coronal (left), sagittal (center), and horizontal (right) image slices from two representative MPPF-PET studies are shown superimposed on the rat brain atlas following registration with a synthetic PET target: (a) synthetic PET target MPPF5, (b) and (c) representative PET studies. The cross-hairs cover the same point on the atlas in all images.

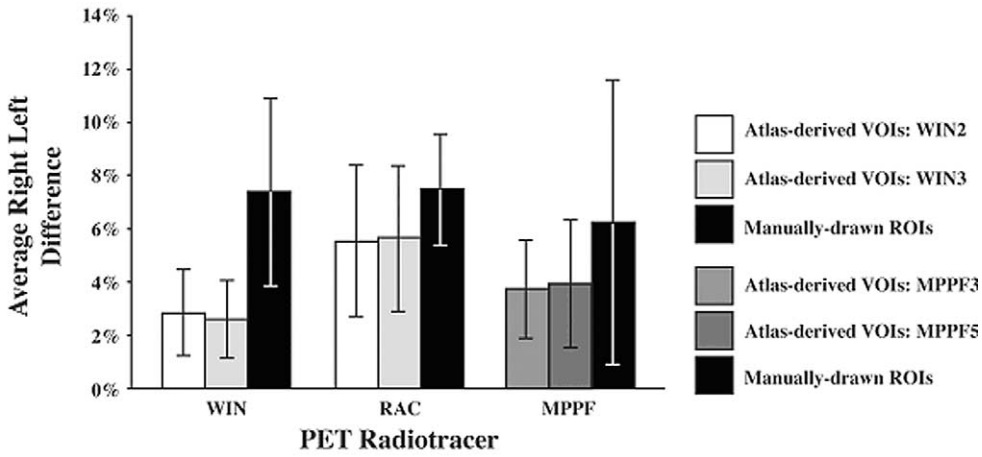


Fig. 12. The average right-left difference (±SD) in binding ratio measured with atlas-derived VOIs and manually drawn ROIs are displayed for each radiotracer.

targets that achieved registration of all corresponding PET studies with no obvious failures all had nonzero voxel values assigned throughout the entire brain.

The amount of smoothing applied to the synthetic PET target did not affect the number of obvious registration errors, indicating that the spatial resolution of the PET studies need not be known to submillimeter accuracy in creating an appropriate synthetic PET target. In contrast, the initial position of the PET study relative to that of the synthetic PET target was shown to be a major factor in registration. Accordingly, a spatial transformation must be performed on each PET study prior to registration, to align the PET study with the synthetic PET target within ~5 mm, such that obvious registration failure will not occur. While this can be easily achieved by visual alignment of the image volumes, for an automated system, it is necessary to place all images within this range with the same initial transformation. This requires that image volumes of the PET studies be spatially aligned with each other prior to analysis. Such desired accuracy can be readily achieved by reproducibly positioning the rat brain within the PET scanner with the use of a stereotactic frame (Rubins et al., 2001).

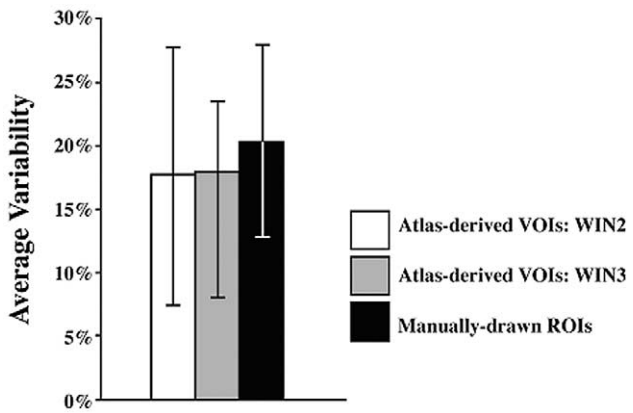


Fig. 13. The average variability (difference/mean) of binding ratios measured in repeat WIN-PET studies of the same subjects with atlas-derived VOIs and with manually drawn ROIs are displayed.

For all PET studies evaluated, the radioactivity concentration measured by this method for the structure of highest radioactivity concentration was within 2% of the maximum radioactivity measurement possible with that VOI. The small differences between these values could easily have been caused by factors unrelated to registration, such as small differences in radioactivity concentration in the region surrounding the brain structure, resulting in nonsymmetrical spillover of measured radioactivity into the VOI. These results imply that once a PET study was registered with a synthetic PET target without obvious registration failure, good alignment was achieved between the designated brain structure and corresponding VOI. For routine use of this analysis method with radiotracers that primarily accumulate in one brain structure, such a comparison can be used to ensure registration accuracy.

Measurements of radioligand binding calculated from radioactivity concentration measurements obtained with atlas-derived VOIs were more precise than those calculated with radioactivity concentration measurements obtained with single-plane, manually- drawn ROIs for all comparisons. These results indicate that the atlas-derived VOI method not only provides numerous practical advantages over manual ROI methods, but will also improve the precision of radioactivity concentration measurements.

It was observed in these evaluations that WIN- and RAC-PET studies could be registered to synthetic PET targets over a wider range of conditions than MPPF-PET studies. One contributing factor was that the WIN- and RAC-PET studies were obtained over an extended axial field of view, and thus resultant image volumes contained nearly twice as much of the brain as in MPPF-PET studies. This may indicate that the amount of the brain placed within the PET scanner field of view is an important factor in

registration to a synthetic PET target. However, it will not be an issue for most investigators, since commercial small-animal PET scanners such as the microPET P4 scanner (Concorde, Inc., Knoxville, TN, USA) (Tai et al., 2001) have a large enough axial field of view to accommodate the entire rat brain in a single imaging position. Another relevant factor was that radioactivity concentrations within the brain relative to surrounding regions were higher for WIN- and RAC-PET studies but were similar for MPPF-PET studies. As the assignment of nonzero voxel values to the entire brain region of synthetic PET targets was shown to be important for registration, it is therefore likely that a higher radioactivity concentration within the brain than in surrounding regions facilitates accurate registration of PET studies. This could become a more significant issue with new, highly selective radioligands that clear quickly from the brain when not specifically bound to the receptor of interest. In such cases, it may be possible to use data summed only over the early portion of the PET study for registration to a synthetic PET target, as radioactivity concentration in brain is likely to be greater than in surrounding regions during that time period.

Overall, the results of this evaluation indicate that this analysis method produces accurate alignment of brain structures and corresponding VOIs in PET studies of multiple subjects, obtained with various radiotracers and under various experimental conditions, and that this method provides a superior alternative to manual ROI methods. As a unique synthetic PET target can be constructed for use with each radiotracer and specific set of experimental conditions, these results also imply that the method can be applied to a wide range of in vivo imaging studies of the rat brain. However, it should be noted that the application of this method to any type of PET study other than those included in this evaluation will first require further validation of the method.

An important next step in the development of this method is to include correction for the partial volume effect (PVE). This effect, caused by the limited spatial resolution of PET scanners, can result in errors in radioactivity measurements for any structure with a diameter less than 2× the spatial resolution of the PET scanner (Hoffman et al., 1979). The geometric transform matrix (GTM) method, requiring a segmented MRI image volume, has been developed for PVE correction in human brain PET studies (Rousset et al., 1998; Slifstein et al., 2000). The atlas-derived VOIs could likewise be applied for PVE correction in rat brain PET studies. Additional refinements may also improve the performance of this method. For example, a scaling factor can be included in the registration of PET studies and synthethic PET targets, potentially making possible the application of this methodology to animals of a wider weight range than with the current rigid-body registrations. As new, higher resolution PET scanners become available, a more detailed analysis of the rat brain can be obtained by including VOIs for smaller brain structures, and similar analysis methods can also be developed for brain studies of smaller species, such as the mouse.

## Acknowledgments

The authors wish to thank Colin Studholme for providing MI image registration software and for many helpful discussions, Roger Woods for providing AIR registration software, Arthur Toga and Paul Thompson for providing the anatomical rat brain dataset, Linda Shultz for performing nigrostriatal lesion procedures, and Judy Edwards and Waldimar Ladno for assistance with microPET procedures. This research was supported by the Office of Science (BER), U.S. Department of Energy, Cooperative Agreement No. DE-FC03-02ER63420, and National Institutes of Health Grant R01 EB00561.

## References

Ait Amara, D., Segu, L., Buhot, M.C., 2001. Region-specific decrease in 5-HT1A and 5-HT1B binding sites after intra-hippocampal ibotenic acid injections in the rat. Neurosci. Lett. 310, 25–28.

Ardekani, B.A., Braun, M., Hutton, B.F., Kanno, I., Iida, H., 1995. A fully automatic multimodality image registration algorithm. J. Comput. Assist. Tomogr. 19, 615–623.

Bauer, B., Wagner, R., 1994. Production of [11C]raclopride with high specific activity for clinical use. J. Labelled Comput. Radiopharm. 35, 464–465.

Bohm, C., Greitz, T., Blomqvist, G., Farde, L., Forsgren, P.O., Kingsley, D., Sjogren, I., Wiesel, F., Wik, G., 1986. Applications of a computerized adjustable brain atlas in positron emission tomography. Acta. Radiol. Suppl. 369, 449–452.

Brownell, A.L., Elmaleh, D.R., Meltzer, P.C., Shoup, T.M., Brownell, G.L., Fischman, A.J., Madras, B.K., 1996. Cocaine congeners as PET imaging probes for dopamine terminals. J. Nucl. Med. 37, 1186–1192.

Chatziioannou, A., Qi, J., Moore, A., Annala, A., Nguyen, K., Leahy, R., Cherry, S.R., 2000. Comparison of 3-D maximum a posteriori and filtered backprojection algorithms for high-resolution animal imaging with microPET. IEEE Trans. Med. Imaging 19, 507–512.

Cherry, S.R., Shao, Y., Silverman, R.W., Meadors, K., Siegel, S., Chatzioannou, A., Young, J.W., Jones, W., Moyers, J.C., Newport, D., Boutefnouchet, A., Farquhar, T.H., Andreaco, M., Paulus, M.J., Binkley, D.M., Nutt, R., Phelps, M.E., 1997. MicroPET: a high resolution PET scanner for imaging small animals. IEEE Trans. Nucl. Sci. 44, 1161–1166.

Cicchetti, F., Brownell, A.L., Williams, K., Chen, Y.I., Livni, E., Isacson, O., 2002. Neuroinflammation of the nigrostriatal pathway during progressive 6-OHDA dopamine degeneration in rats monitored by immunohistochemistry and PET imaging. Eur. J. Neurosci. 15, 991–998.

Cohen, A.D., Tillerson, J.L., Smith, A.D., Schallert, T., Zigmond, M.J., 2003. Neuroprotective effects of prior limb use in 6-hydroxydopamine-treated rats: possible role of GDNF. J. Neurochem. 85, 299–305.

Farde, L., Hall, H., Ehrin, E., Sedvall, G., 1986. Quantitative analysis of D2 dopamine receptor binding in the living human brain by PET. Science 231, 258–261.

Hayakawa, N., Uemura, K., Ishiwata, K., Shimada, Y., Ogi, N., Nagaoka, T., Toyama, H., Oda, K., Tanaka, A., Endo, K., Senda, M., 2000. A PET-MRI registration technique for PET studies of the rat brain. Nucl. Med. Biol. 27, 121–125.

Hoffman, E.J., Huang, S.C., Phelps, M.E., 1979. Quantitation in positron emission computed tomography: 1. Effect of object size. J. Comput. Assist. Tomogr. 3, 299–308.

Maes, F., Collignon, A., Vandermeulen, D., Marchal, G., Suetens, P., 1997. Multimodality image registration by maximization of mutual information. IEEE Trans. Med. Imaging 16, 187–198.

Melega, W.P., Lacan, G., Desalles, A.A., Phelps, M.E., 2000. Long-term methamphetamine-induced decreases of [(11)C]WIN 35,428 binding in striatum are reduced by GDNF: PET studies in the vervet monkey. Synapse 35, 243–249.

Minoshima, S., Koeppe, R.A., Frey, K.A., Ishihara, M., Kuhl, D.E., 1994. Stereotactic PET atlas of the human brain: aid for visual interpretation of functional brain images. J. Nucl. Med. 35, 949–954.

Nikolaus, S., Larisch, R., Beu, M., Forutan, F., Vosberg, H., Muller-Gartner, H.W., 2003. Bilateral increase in striatal dopamine D(2) receptor density in the 6-hydroxydopamine-lesioned rat: a serial in vivo investigation with small animal PET. Eur. J. Nucl. Med. Mol. Imaging 30, 390–395.

Paxinos, G., Watson, C., 1986. The Rat Brain in Stereotaxic Coordinates, second ed. Academic Press, Sydney.

Paxinos, G., Watson, C., Pennisi, M., Topple, A., 1985. Bregma, lambda and the interaural midpoint in stereotaxic surgery with rats of different sex, strain and weight. J. Neurosci. Methods 13, 139–143.

Pelizzari, C.A., Chen, G.T., Spelbring, D.R., Weichselbaum, R.R., Chen, C.T., 1989. Accurate three-dimensional registration of CT, PET, and/or MR images of the brain. J. Comput. Assist. Tomogr. 13, 20–26.

Plenevaux, A., Lemaire, C., Aerts, J., Lacan, G., Rubins, D., Melega, W.P., Brihaye, C., Degueldre, C., Fuchs, S., Salmon, E., Maquet, P., Laureys, S., Damhaut, P., Weissmann, D., Le Bars, D., Pujol, J.F., Luxen, A., 2000. [(18)F]p-MPPF: a radiolabeled antagonist for the study of 5-HT(1A) receptors with PET. Nucl. Med. Biol. 27, 467–471.

Press, W.H., Teukolsky, S.A., Vettering, W.T., Flannery, B.P., 1997. Numerical Recipes in C: The Art of Scientific Computing, second ed. Cambridge University Press, Cambridge.

Qi, J., Leahy, R.M., Cherry, S.R., Chatziioannou, A., Farquhar, T.H., 1998. High-resolution 3D bayesian image reconstruction using the microPET small-animal scanner. Phys. Med. Biol. 43, 1001–1013.

Rousset, O.G., Ma, Y., Evans, A.C., 1998. Correction for partial volume effects in PET: principle and validation. J. Nucl. Med. 39, 904–911.

Rubins, D.J., Meadors, A.K., Yee, S., Melega, W.P., Cherry, S.R., 2001. Evaluation of a stereotactic frame for repositioning of the rat brain in serial PET imaging studies. J. Neurosci. Methods 107, 63–70.

Schaltenbrand, G., Wahren, W., 1977. Atlas for Stereotaxy of the Human Brain. Georg Thieme Verlag, Stuttgart.

Siegel, S., Dahlbom, M., 1992. Implementation and evaluation of a calculated attenuation correction for PET. IEEE Trans. Nucl. Sci. 39, 1117–1121.

Slifstein, M., Mawlawi, O., Lauruelle, M., 2000. Partial volume effect correction: Methodological considerations, in: Paulson, O. (Ed.), Physiological Imaging of the Brain with PET, Academic Press, San Diego, pp. 65–71.

Studholme, C., Hill, D.L., Hawkes, D.J., 1997. Automated three-dimensional registration of magnetic resonance and positron emission tomography brain images by multiresolution optimization of voxel similarity measures. Med. Phys. 24, 25–35.

Swanson, L.W., 1992. Brain Maps: Structure of the Rat Brain. Elsevier, Amsterdam.

Tai, C., Chatziioannou, A., Siegel, S., Young, J., Newport, D., Goble, R.N., Nutt, R.E., Cherry, S.R., 2001. Performance evaluation of the microPET P4: a PET system dedicated to animal imaging. Phys. Med. Biol. 46, 1845–1862.

Talairach, J., Tournoux, P., 1988. Co-Planar Stereotaxic Atlas of the Human Brain: 3-Dimensional Proportional System: An Approach to Cerebral Imaging by Jean Talairach and Pierre Tournoux; Translated by Mark Rayport. Thieme Medical Publishers, New York.

Thompson, P.M., Woods, R.P., Mega, M.S., Toga, A.W., 2000. Mathematical/computational challenges in creating deformable and probabilistic atlases of the human brain. Hum. Brain. Mapp. 9, 81–92.

Toga, A.W., Santori, E.M., Hazani, R., Ambach, K., 1995. A 3D digital map of rat brain. Brain. Res. Bull. 38, 77–85.

Wells 3rd, W.M., Viola, P., Atsumi, H., Nakajima, S., Kikinis, R., 1996. Multi-modal volume registration by maximization of mutual information. Med. Image Anal. 1, 35–51.

Wilson, A.A., DaSilva, J.N., Houle, S., 1996. In vivo evaluation of [11C]- and [18F]-labelled cocaine analogues as potential dopamine transporter ligands for positron emission tomography. Nucl. Med. Biol. 23, 141–146.

Woods, R.P., Cherry, S.R., Mazziotta, J.C., 1992. Rapid automated algorithm for aligning and reslicing PET images. J. Comput. Assist. Tomogr. 16, 620–633.

Woods, R.P., Grafton, S.T., Holmes, C.J., Cherry, S.R., Mazziotta, J.C., 1998a. Automated image registration: I. General methods and intrasubject, intramodality validation. J. Comput. Assist. Tomogr. 22, 139–152.

Woods, R.P., Grafton, S.T., Watson, J.D., Sicotte, N.L., Mazziotta, J.C., 1998b. Automated image registration: II. Intersubject validation of linear and nonlinear models. J. Comput. Assist. Tomogr. 22, 153–165.

Woods, R.P., Mazziotta, J.C., Cherry, S.R., 1993. MRI-PET registration with automated algorithm. J. Comput. Assist. Tomogr. 17, 536–546.